Physical Communication 49 (2021) 101482

Contents lists available at ScienceDirect

Physical Communication

journal homepage: www.elsevier.com/locate/phycom

Full length article

Random sampling for effective spectrum sensing in cognitive radio time slotted environment

Salvatore Serrano [a], Marco Scarpa [a,*,1], Asmaa Maali [b], Abdallah Soulmani [b], Najib Boumaaz [b]

[a] Department of Engineering, University of Messina, C.da Di Dio - Villaggio S. Agata, 98166 Messina, Italy
[b] Laboratory of Electrical Systems, Energy Efficiency, and Telecommunications (LSEEET), Department of Physics, Faculty of Sciences and Technologies, Cadi Ayyad University, Marrakech, Morocco

ARTICLE INFO

Article history:
Received 27 May 2020
Received in revised form 11 October 2021
Accepted 11 October 2021
Available online 21 October 2021

Keywords:
Cognitive radio
Spectrum sensing
Random sampling
Classification
Neural network
GSM

ABSTRACT

In the context of wireless communication, Cognitive Radio has been proposed to ensure an optimal use of the spectrum. It divides the communication transceivers into two categories. Primary User has the priority to use the spectrum band while secondary user is an opportunistic user that can transmit on that band whenever it is available. In order to determine whether a concerned band is occupied or vacant, spectrum sensing functionality is needed together with an appropriate algorithm able to analyze the produced data in order to understand whether a primary user is transmitting or not. In this paper, we contribute by investigating a narrowband spectrum sensing based on two proposed parameters obtained randomly sampling the signal and a Multilayer Perceptron neural network (MLP) classifier. We show that the use of random sampling is more effective than the use of classical uniform sampling. We analyzed the activity status in the GSM channel by using a synthetically generated signal: the signal has been sampled using both uniform and random sampling, than it has been reconstructed and finally classified with the aim of a neural network based classifier. The performances in terms of Receiver Operating Characteristic curves for different Signal to Noise Ratio are presented.

1. Introduction

Software Defined Radio (SDR) and cognitive radio (CR) technologies are considered as important innovations in wireless communications and are expected to play an important role in the future 5G networks [1]. SDR is a multi-mode, multi-standard, and configurable system where some radio functions usually implemented in hardware are converted to software. In such systems, the software processing is used within the radio device to implement operating functions. The challenge of an SDR system is to deal with the need of high sample rates and the need of very selective filters treating large bands [2]. Therefore, the idea of using the random sampling in that system offers more flexibility in sampling frequencies choices [3,4]. Given the need for more efficient use of the spectrum resource, CR uses SDR technology while attempting to dynamically manage the radio spectrum. A cognitive radio monitors locally the radio spectrum to determine regions that are not occupied by their assigned users and transmits in those bands. In CR system, primary users (PU) can be defined as the users who have higher priority in the usage of a specific frequency band. Secondary users (SU) are ones who have lower priority [5]; they use the frequency band in such a way they do not interfere with primary users. In this context, Spectrum Sensing (SS) is a crucial function and one of the most challenging issues in cognitive radio systems. This ability of sensing the spectrum makes CR innovative with respect to the other kinds of radios applications. Recently, the Federal Communication Commission (FCC) has developed new spectrum policies to permit an opportunistic access by SUs to a licensed band when PUs are absent [6]. As we noticed above, one of the key functions of cognitive radio is the spectrum sensing which is the most important skill to establish cognitive radio networks. It aims to determine the availability of the spectrum and to detect the presence of a primary user when a user operates in a licensed band. In general, Cognitive Radio Networks (CRN) can be divided into three different approaches depending on the nature of interaction between the SU and PU. In the first one, denoted as *interweave network*, SUs are not allowed to access the band when a PU is active; in the second one, called *underlay*, the SUs enter the PUs only when their activity will not cause considerable interference or capacity penalty to the PU. Thus, they can share the spectrum but PUs have a higher priority than SUs.

* Corresponding author.
E-mail addresses: sserrano@unime.it (S. Serrano), mscarpa@unime.it (M. Scarpa), asmaa.maali@ced.uca.ma (A. Maali), a.soulmani@uca.ma (A. Soulmani), n.boumaaz@uca.ma (N. Boumaaz).
[1] IEEE member, membership number 94227397.

https://doi.org/10.1016/j.phycom.2021.101482
1874-4907/

Moreover, in the third one, called *overlay*, both PUs and SUs can transmit concurrently [6]. However, using overlay, the SU devices must have knowledge about the PU transmitted data sequence encoding methods. This information can be used to cancel the PU interference on SU receivers (using canceling techniques such as dirty paper coding) or by SU nodes to cooperate with the primary network by relaying PU messages [7].

In the present work, we will consider interweave CRN only. In such a context, sampling the spectrum is not enough for opportunistically using the band; a user detection algorithm is needed in order to understand if a primary user is transmitting or not directly from the sampled signal. The goodness of such a kind of algorithm in fact affects system performances [8]. Whereas cognitive radio is usually applied in a spectrum environment characterized by long-term steady-state conditions, at the opposite, we propose an approach which makes it possible to apply cognitive radio in a spectrum environment characterized by fast variations of the channel occupancy state.

The paper is organized as in the following: Section 2 discusses related works and introduces the scenario we use as reference. In Section 3, the random sampling is introduced together with the reconstruction theory starting from a randomly sampled sequence. Section 4 presents the parameters we propose in the context of narrowband spectrum sensing with the purpose to identify the presence of PUs. Section 5 evaluates the performance of the proposed work in terms of PU detection by means of neural network classifier. Finally, conclusions are drawn in Section 6.

2. Reference scenario and related work

As revealed by FCC, the radio spectrum utilization in the band below 3 GHz can vary from 15% to 85%. This low utilization of the radio spectrum has meant that industrial standardization bodies (IEEE 802.22, IEEE 802.11af, Ecma-392) have preferred interweave CRN. In addition, interweave paradigm can guarantee a reasonable Quality-of-Service (QoS) due to the fact that it is possible to provide sufficient reliability. In this scenario, spectrum sensing can be classified according to the size of the observed band: Wide band spectrum sensing (WBSS) tries to identify the portions (sub-bands) of the observed band which are busy due to the signal transmission of PUs and those which are free. Narrowband spectrum sensing (NBSS) considers only a specific portion of the band trying to identify whether it is busy or free. In interweave networks with NBSS, a SU has to sense the spectrum in order to detect whether it is busy by a PU or not. Moreover, after it decided to begin its transmission, the SU has to monitor the spectrum in order to detect if a PU decided to start its transmission. When this condition occurs, the SU has to quickly vacate the occupied spectrum. Several wireless medium access protocols act in a time slotted fashion. Specifically, it occurs by using a periodic time division multiple access (for example in GSM networks) or a statistical time division multiplexing (for example in IEEE 802.11 wireless networks). Infrastructure networks, in the context of IEEE 802.11, are established using Access Points (APs). The AP is analogous to the base station in a GSM network. Anyway, in both cases the beginning of PU's transmission is synchronized with the boundary of the timeslots. If an SU is able to identify the boundaries of timeslots, it can sense the spectrum at their beginning, thus it can start the transmission when the spectrum appears vacant and stops it before the end of the current slot. Using this approach, the monitoring step of the spectrum is not necessary and the collision rate with PU will be related only to errors in the decision task of the sensing.

A lot of works on spectrum sensing have been published. In [3,9], the authors presented the association of the energy detector and maximum eigenvalue detector with random sampling; they studied this approach in terms of ROC curves, and they showed the utility of the random sampling in the context of cognitive radio compared to uniform sampling. As far as we know, there are other works on spectrum sensing but they applied the uniform sampling [2,10]. Thus, there are works in the context of cognitive radio applying MultiLayer Perceptron (MLP) for prediction but they do not address the issue of non-uniform sampling [11,12]. These works considerably differ from ours. Specifically, in [11], the authors propose a MLP able to predict the power strength in a GSM channel with a time sweep of 157 seconds and based on the knowledge of the time series of the signal. In our approach, we exploit MLP in order to establish if a single GSM time slot is free or busy just analyzing only one half of the time slot signal. The authors of [12] assume a single primary channel whose state information (CSI) is used by the system for learning based prediction of future primary activity. They consider a slot-wise PU traffic and compare different ML techniques (Multilayer Perceptron, Recurrent Neural Networks, Linear and Gaussian Support Vector Machines) in three different traffic scenarios (Poisson, Interrupted-Poisson and Self-similar traffic). In this context, the use of ML is completely different from ours because the prediction is made using the past values of the CSI and not an estimation of the power spectral density in the current slot.

As it is known, the spectrum sensing in cognitive radio system requires high sampling rate, high-resolution analog to digital converters with large dynamic range, and high-speed signal processors. Therefore, it is difficult to implement this function if the hardware does not satisfy such strict criteria. Therefore, the application of a random sampling sequence in cognitive radio systems offers several advantages compared to the uniform sampling case [3,13]: (1) there is more flexibility in sampling frequencies, (2) the constraints on signal filtering operation are reduced and (3) the aliases of the spectrum are attenuated [14] (or completely eliminated in the case of a stationary sampling sequence). According to the classification proposed in [6], "random sampling" can be used to perform SubNyquist based WBSS by means of Digital Compressive Sensing. Compressive sensing (CS) can guarantee the recovery accuracy of suitably constrained signals by using sampling rates much lower than the Nyquist limit. CS (also called compressive sampling) differs from Nyquist sampling in that it combines the compression and sampling stages. It utilizes the characteristics of sparse representation of signals on a set of bases and achieves the perception of high-dimensional signals through non-correlated observations of low-dimensional space, low-resolution, and under-Nyquist sampled data to reconstruct the original signal by combining optimization methods. The sparseness of the signal in such domain is a necessary condition for compressive sensing, uncorrelated observation is the key to compressive sensing, and signal reconstruction is the technique of compressively sensing reconstructed signals [15]. One popular way to reduce the sampling rate for the case of multiband signals with a frequency support on a union of finite interval is the Multi-Coset sampling [16]. Another approach consists in applying a modulated wideband converter consisting of multiple branches, each of which employs a different mixing function followed by low-pass filtering and low-rate uniform sampling [17]. Both of the above approaches can be cast into a compressive sampling framework [18]. In [19], based on previous results about Multi-Coset sampling and using the well known Non-Uniform Fourier Transform through Bartlett's method for Power Spectral Density estimation, the authors propose a new smart sampling scheme named "Dynamic Single Branch Non-uniform Sampler". In [20], the authors propose a survey on compressive sensing techniques applied to cognitive radio networks, while a review on Sub-Nyquist wideband spectrum sensing techniques for cognitive radio is introduced in [21], and, contextually, two new

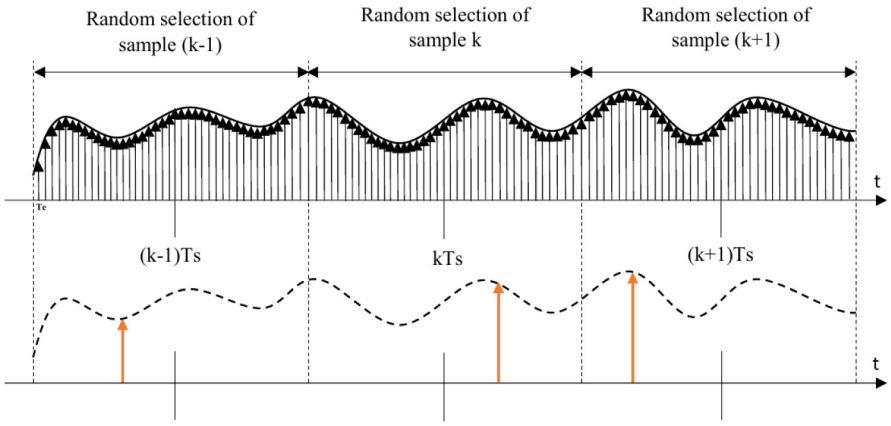

Fig. 1. The random sampling is performed by taking a sample; we apply a random sequence centered at $k \cdot T_s$.

techniques, based on Multi-Coset sampling and on modulated wideband converter, are proposed. They claim that various open challenges need to be still addressed in existing sub-Nyquist sensing techniques, including: (1) existing sub-Nyquist techniques require the wideband signal to be sparse in the frequency domain; (2) the existing CS techniques require knowledge about sparsity but in a real context the sparsity level may be either unknown or time-varying.

In this work, we propose a NBSS using random sampling in a time-varying scenario where, with reference to the recent work proposed in this context, the idea is to study the feasibility of performing spectrum sensing with the following requirements:

1. using a sub-Nyquist sampling rate without filtering the narrowband of the signal;
2. synchronizing the start of the sampled period with the boundary of the PU transmission time slot;
3. using only less than half of the samples acquired in a time slot in order to have time room to perform some SU transmission in the second half of the time slot.

At the best of our knowledge, such strict requirements have not been considered in the other related works. To obtain this goal, we propose a set of two new features extracted from the PSD of the rebuilt sampled signal (using random sampling) and a busy/free classifier based on neural networks. We took into account the GSM signal as PUs' time slotted transmission environment. Specifically, we synthesized a complex wideband passband GSM signal wide 2 MHz containing 10 channels of 200 kHz; we sampled it at 2 MHz rate and, without applying any filter, we downsampled the sequence with an average rate of 200 kHz (using both random and uniform distribution of the samples) in order to obtain the central channel. As known, this downsampling will generate an aliasing effect of the adjacent channels that we try to bypass by the use of random sampling. Definitively, we can consider a 2 MHz bandwidth signal downsampled at an average rate of 200 kHz. In the case of random sampling, as presented in Fig. 1, the sampling time instants are chosen as follow: The $k-th$ random sampling instant is set by using a random distribution centered at $k \cdot T_s$, with $T_s = T_e \cdot K$, where T_e is the input sampling period and K is the decimation factor (we chose $K = 10$). As well known, random sampling guarantees to bypass the aliasing effect generated by downsampling. Practically, uniform downsampling is equivalent to sampling with a rate necessary to sample a single channel but using a not suitable antialiasing filter before the sampling unit. As known from the sampling theory, in order to avoid aliasing, we need to filter the analog signal by inserting a suitable antialiasing filter before the sampling unit. The analog filter suitable in the application we are focusing on,

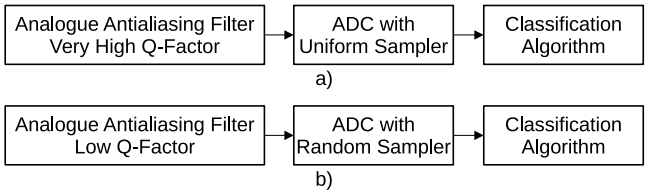

Fig. 2. Cascade of functional blocks to perform narrowband spectrum sensing using uniform (a) and proposed random sampling (b).

taking into account that the central frequency is very high (in the case of GSM about 1.8 GHz), has a very high Q-factor. When our target is to perform spectrum sensing in a narrowband channel of 200 kHz (i.e., evaluate if the channel is busy or not), we show that, using our approach based on random sampling, it is possible to use, with some specific constraints, a filter having a lower Q-Factor of one-order of magnitude (Fig. 2). We stress the fact that cognitive radio is usually applied in a spectrum environment characterized by long-term steady-state conditions. Our purpose instead is to show that it is possible to apply cognitive radio in a spectrum environment characterized by fast variations of the channel occupancy state using random sampling, a new set of parameters and classification based on a multilayer perceptron, that, at the best of our knowledge, are not used before together in similar environments.

Flowchart in Fig. 3 shows the steps of the proposed mechanism: the wideband signal acquisition by means of sub-Nyquist random sampling starts at boundaries of GSM time slot and lasts for one half of a time slot; given the random samples, the signal rebuilding and the evaluation of PSD will start; the proposed parameters are extracted from the PSD, and they are used as inputs of the free/busy classifier who will take a decision for the current time slot. Based on the classifier response, the SU should be able to take a decision on the channel usage in the remaining portion of the timeslot.

We chose GSM as a test signal because it is currently considered as the most successful cellular standards and has the highest market share among all cellular technologies. This innovation plays an increasingly important role in modern world and in people's social lives. Most of the people over the world use mobile devices as a tool for communicating with each other. Our interest in using GSM infrastructure is mainly motivated by the extensive demands for using the 800 - 900 MHz bands by NarrowBand IoT (NB-IoT) devices [22], and the under-utilization of this band [23]. In fact, deploying NB-IoT in such frequency bands is a great choice because they provide an already large and established ecosystem

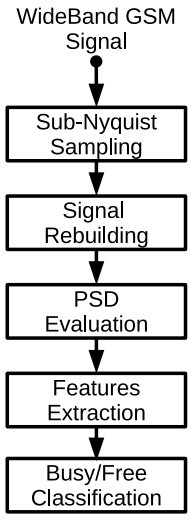

Fig. 3. Flow Chart of the proposed SS approach.

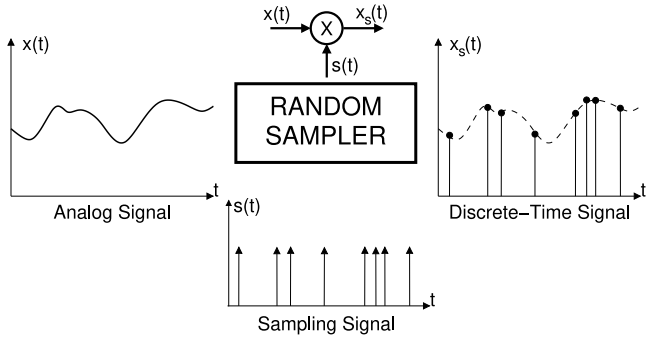

Fig. 4. Random Sampling Principle.

and extensive coverage capabilities [24]. They also have excellent propagation characteristics, which generally improves the indoor penetration [25].

3. Random sampling and reconstruction theory

Random sampling process consists in converting a continuous analog signal $x(t)$ into a discrete time representation $x_s[n]$ (Fig. 4) where the sampling instants are not uniformly distributed.

The application of the random sampling gives a large flexibility in sampling rates choice and makes it possible to reduce, or to eliminate, in the case of a stationary sequence, the aliases of spectrum [26,27], helping in reducing the constraints on the various components of the transmission chain.

In the literature, there are two most commonly used random sampling modes namely Additive Random Sampling (ARS) and Jitter Random Sampling (JRS) [28]. The Jittered Random Sampling (JRS) is a random process where the sampling times are described by the following expression:

$$t_n = nT + \tau, \qquad T > 0, n = 1, 2, \ldots \tag{1}$$

where T represents the mean sampling period and τ is a uniform distributed random variable in $[0, T[$. The Additive Random Sampling (ARS) has been originally proposed in [29] by Shapiro and Silverm as an approach for randomly sampling signal in order to avoid aliasing phenomena (alias-free). This mode can be described by the following time sequence:

$$t_n = t_{n-1} + \tau, \qquad n = 1, 2, \ldots \tag{2}$$

where τ denotes a random variable with a probability density function $f_\tau(t)$, a variance σ_τ^2 and a mean μ_τ; the most used distributions are the uniform and the normal distributions. It is important to point out that $T = \mu_\tau = \frac{1}{f_s}$ where f_s is the average rate of the random sampled signal.

In this contribution, we have been interested in experimenting the JRS mode, thus we have implemented and used it in our experimentation (Section 5).

Several reconstruction techniques of randomly sampled signals have been presented in the literature [30]. In this work, we used the Adaptive-weight Conjugate gradient Toeplitz algorithm to reconstruct our signal from its non-uniform samples, and we compared it with the direct method of Singular Value Decomposition Algorithm [30].

3.1. Singular value decomposition algorithm (SVD)

Let us assume the signal $x(t)$ is observed and N samples are stored into a column vector denoted as $\mathbf{x}_s$, i.e.

$$\mathbf{x}_s = (x(t_1), x(t_2), \ldots, x(t_N))^T = (x_s[1], x_s[2], \ldots, x_s[N])^T .$$

When a sample rate higher than the double of the effective bandwidth is used (Nyquist frequency is higher than the effective bandwidth), an $M < N$-dimensional orthogonal basis, made by complex exponential functions, can be identified [13], and the signal can be written as their linear combination:

$$x(t) = \sum_{k=1}^{M} c_k e^{2\pi \jmath f_k t}, \ \forall t > 0 \tag{3}$$

where the f_k, $k = 1, \ldots, M$ are frequencies components in the signal bandwidth and the c_k are appropriate unknown constant values. Of course, Eq. (3) is valid also for samples in $\mathbf{x}_s$, thus

$$x(t_i) = \sum_{k=1}^{M} c_k e^{2\pi \jmath f_k t_i}, \ i = 1, \ldots, N. \tag{4}$$

Eq. (4) can be written in matrix form as

$$\mathbf{x}_s = \mathbf{A} \cdot \mathbf{c} \tag{5}$$

where the generic element of $\mathbf{A}$ is defined as $A_{ik} = e^{2\pi \jmath f_k t_i}$. We put in evidence that when the signal is not under sampled, as usual, $M \leq N$ holds, i.e the basis dimension is less than the number of samples.

The knowledge of the coefficients c_k gives a methodology to reconstruct the signal through the Eq. (3). They can be estimated by minimizing the squared error in the following problem derived by Eq. (5):

$$\min_{\hat{\mathbf{c}}}\{E_q^2\} = \min_{\hat{\mathbf{c}}}\{|\mathbf{A} \cdot \hat{\mathbf{c}} - \mathbf{x}_s|^2\} \tag{6}$$

where we used the notation $\hat{\mathbf{c}}$ to stress the fact that the computed values are not the real values of Eq. (4) but an estimation of them. As a consequence, when they will be used in place of $\mathbf{c}$, the reconstructed estimated signal $\hat{\mathbf{x}}_s = \mathbf{A} \cdot \hat{\mathbf{c}}$ will be affected by an error.

To solve the problem in (6) is equivalent to solve the following system of linear equation[2]:

$$\mathbf{A}^* \cdot \ \mathbf{A} \cdot \hat{\mathbf{c}} = \mathbf{A}^* \cdot \ \mathbf{x}_s \tag{7}$$

The SVD approach helps in efficiently solving the system (7). In fact, according to it, the matrix $\mathbf{A}$ is factorized into

$$\mathbf{A} = \mathbf{U} \cdot \mathbf{S} \cdot \mathbf{V}^* \tag{8}$$

where

[2] The symbol $\mathbf{B}^*$ denotes the conjugate transpose of the matrix $\mathbf{B}$

- **U** is a $N \times N$ complex unitary matrix[3];
- **S** is an $M \times N$ diagonal matrix, and $\mathbf{S} = diag\left(\sigma_1, \sigma_2, \ldots \sigma_p\right)$, with $p = min\,(M, N)$; the σ_is are known as singular values and verifies $\sigma_1 \geq \sigma_2 \geq \cdots \geq \sigma_p \geq 0$;
- **V** is an $M \times M$ unitary matrix.

By bringing in position $\mathbf{Z} = \mathbf{V}^* \cdot \hat{\mathbf{c}}$ and $\mathbf{Y} = \mathbf{S}^* \cdot \mathbf{U}^* \cdot \mathbf{x}_s$, the Eq. (7) is rewritten into:

$$\mathbf{S}^* \cdot \mathbf{S} \cdot \mathbf{Z} = \mathbf{Y} \tag{9}$$

from which

$$z_k = \frac{y_k}{s_{kk}^2}, \ k = 1, \ldots, p.$$

By putting this latter values back to the introduced position, the c_k are easily computed as

$$\hat{\mathbf{c}} = \mathbf{V} \cdot \mathbf{Z}.$$

The $\hat{c}_k$ values can now be used in Eq. (3), and the signal can be recovered and compared to the original one by using the following formula:

$$E_m^2 = \frac{\sum_k \left|x(t_k) - \hat{x}(t_k)\right|^2}{\sum_k |x(t_k)|^2}$$

3.2. Adaptive-weight conjugate gradient Toeplitz (ACT)

The ACT is an iterative reconstruction algorithm of randomly sampled signals. It arises by combining the adaptive weights method formulated in [31,32] with the fast iterative solution of Toeplitz systems based on circulant matrices by the conjugate gradient (CG) method. This method is very efficient for reconstructing randomly sampled signals due to its accuracy and speed. With the aim of facilitating reading, we summarize the fundamental steps of this methodology below.

The reconstruction of a sequence $x[n]$ from its irregular samples using the ACT iterative algorithm as presented in [31] is equivalent to the solution of $\mathbf{A}_\omega \mathbf{y} = \mathbf{b}$, where $\mathbf{A}_\omega$ is a $(2M+1) \times (2M+1)$ Toeplitz matrix and M is the bandwidth of the sequence.

Assuming $x[n]$ is a discrete sequence of length N with bandwidth M, according to the discrete Fourier transform theory, it is possible to rebuild the sequence using $2M+1$ complex coefficients b_k, with $k = -M, \ldots, 0, \ldots, M$:

$$x[i] = \frac{1}{N} \sum_{k=-M}^{M} b_k e^{j2\pi k \frac{i}{N}}, \ i = 1, \ldots, N \tag{10}$$

Let $p(t)$ be a real function defined as

$$p(t) = \frac{1}{N} \sum_{k=-M}^{M} b_k e^{j2\pi kt} = \sum_{k=-M}^{M} y_k e^{j2\pi kt}; \tag{11}$$

then, the sequence of samples can be written in terms of $p(t)$

$$x[i] = p\left(\frac{i}{N}\right), \ i = 1, 2, \ldots, N, \tag{12}$$

and the problem of identifying the signal is translated into the reconstruction of $p(t)$ from r irregular samples $t_h = \frac{n_h}{N}$, $h = 1, 2, \ldots, r$. This latter problem is taken on by introducing a set of adaptive-weights $\{\omega_h\}_{h=1}^r$ as below

$$\omega_h = \begin{cases} \frac{t_2 - t_r + N}{2} & h = 1 \\ \frac{t_{h+1} - t_{h-1}}{2} & 2 \leq h \leq r-1 \\ \frac{t_1 + N - t_{r-1}}{2} & h = r \end{cases}$$

[3] A matrix **B** is unitary when $\mathbf{B} \cdot \mathbf{B}^* = \mathbf{B}^* \cdot \mathbf{B} = \mathbf{I}$.

and the algorithm defined by the subsequent equations

$$p_0(t) = \sum_{h=1}^{r} p(t_h)\omega_h \sum_{l=-M}^{M} e^{2\pi Jl(t-t_h)}$$
$$p_{n+1}(t) = p_n(t) + \sum_{h=1}^{r} \left(p(t_h) - p_n(t_h)\right) \omega_h \sum_{l=-M}^{M} e^{2\pi Jl(t-t_h)}$$

Evaluating $p(t_h)$ as

$$p(t_h) = \sum_{k=-M}^{M} y_k e^{J2\pi kt_h},$$

it is possible to expand the equations in the algorithm as

$$p(t) = \sum_{h=1}^{r} \sum_{k=-M}^{M} y_k e^{J2\pi kt_h} \omega_h \sum_{l=-M}^{M} e^{2\pi Jl(t-t_h)}$$

and, after some manipulations, as

$$p(t) = \sum_{l=-M}^{M} \left[\sum_{k=-M}^{M} \left(\sum_{h=1}^{r} \omega_h e^{-J2\pi(l-k)t_h} \right) y_k \right] e^{2\pi Jlt}$$

Let $\mathbf{A}_\omega$ the matrix with entries

$$a_{kl} = a_{k-l} = \sum_{h=1}^{r} \omega_h e^{-J2\pi(l-k)t_h} \quad |h|, |k| \leq M$$

it will be

$$a_{kl} = a_{lk}^*$$

$\mathbf{A}_\omega$ will be an Hermitean positive definite Toeplitz matrix and it will be fully determined by the generating sequence

$$\mathbf{a}_{2M} = \{a_0, a_1, \ldots, a_{2M}\}$$

where

$$a_k = \sum_{h=1}^{r} \omega_h e^{-J2\pi t_j \frac{k}{N}}$$

Specifically

$$\mathbf{A}_\omega = \begin{bmatrix} a_0 & a_1 & \ldots & a_{2M-1} & a_{2M} \\ a_1^* & a_0 & \ldots & a_{2M-2} & a_{2M-1} \\ \vdots & \vdots & \vdots & \vdots & \vdots \\ a_{2M}^* & a_{2M-1}^* & \ldots & a_1^* & a_0 \end{bmatrix}$$

Let **b** defined by elements

$$b_k = \sum_{h=1}^{r} p(t_h)\omega_h e^{-J2\pi kt_h}, \quad \forall |k| \leq M$$

substituting the values of $p(t_k)$ in it, we obtain

$$b_k = \sum_{h=1}^{r} \sum_{l=-M}^{M} y_l e^{j2\pi lt_h} \omega_h e^{-J2\pi kt_h} =$$
$$= \sum_{l=-M}^{M} \sum_{h=1}^{r} \omega_h e^{-J2\pi(k-l)t_h} y_l = \sum_{l=-M}^{M} a_{kl}^* y_l$$

and consequently

$$\mathbf{b} = \mathbf{A}_\omega \mathbf{y}$$

Then by computing

$$\mathbf{y} = \mathbf{A}_\omega^{-1} \mathbf{b}$$

and

$$p(t) = \sum_{k=-M}^{M} y_k e^{J2\pi kt}$$

the signal $p(t)$ is rebuilt.

Let now $0 \leq t_1, \leq \cdots \leq t_r \leq N-1$ be a subsequence of $0, 1, \ldots, N-1$. It is possible to define

$$s_\omega[n] = \begin{cases} \frac{\omega_i}{N} & n = t_j \\ 0 & \text{otherwise} \end{cases}$$

$$s_p[n] = \begin{cases} p(n) \cdot \omega_j & n = t_j \\ 0 & \text{otherwise} \end{cases}$$

then the entries of the matrix $\mathbf{A}_\omega$ and the elements of the vector $\mathbf{b}$ can be computed using FFT

$$a_k = \mathcal{F}\{s_\omega[n]\} \quad \text{and} \quad b_k = \mathcal{F}\{s_p[n]\} \quad \text{for } k \leq M$$

Moreover, in algorithm suggested by [31] the Toeplitz matrix is replaced by a zero padded circulant matrix in order to obtain a superfast method for reconstruction of band-limited signal from irregular samples. Zero-padding is applied to get a benefit from the greater speed of fft applied to a sequence containing a number of elements equal to a power of 2. The ACT algorithm can be summarized in the following steps:

1. Compute the weights ω_h, $\forall h = 1 \ldots r$;
2. Calculate the first row $\mathbf{a}_{2M+1}$ of $\mathbf{A}_\omega$;
3. Calculate the right side $\mathbf{b}$;
4. Augment $\mathbf{a}_{2M}$ to obtain a zero-padded circulant matrix and accordingly augment the right side $\mathbf{b}$;
5. Apply the GC method to iteratively solve this system of linear equation;
6. Convert the result using the Inverse Fourier Transform back to the signal space.

4. A new set of parameters for Spectrum Classification

Narrowband spectrum sensing can be made by using single-radio or dual-radio equipment. In single-radio sensing, CR-SUs do not access the spectrum during the sensing period: this period is called the quiet period. Based on the length of the quiet period, the spectrum is efficiency decreased. In a dual-radio approach, one of the radio chain is dedicated to the operation of transmission and reception, while the other chain is dedicated to the spectrum sensing and monitoring. However a single-radio equipment gives advantages in terms of simplicity, low cost and low power consumption and it is currently more taken into consideration. Generally speaking, the problem to be solved consists in deciding whether a particular timeslot is "available" or not for the SU transmission. In order to test our approach, we considered a scenario where a PU sampled signal $x_{PU}[n]$ is observed by the SU receiver in presence of an Additive White Gaussian Noise (AWGN) $w[n]$ with mean equal to 0 and variance equal to σ_w^2. Our goal is to exhibit the feasibility of the SS function using a random sampling mode.

As the first phase, we synthetically generated a GSM signal using Octave. We produced a stream of complex samples simulating, through Octave [33], the output of a GSM transmitter that has in input a sequence of random bits. Moreover, in order to take into account the AWGN at the receiver, we added a random value obtained from a gaussian distribution with null mean and variance set according to the desired SNR. Specifically, in order to obtain decimation, we generated oversampled signals with a sample rate equal to $K \cdot f_s$, where f_s is the mean sample rate such that $T_s = \frac{1}{f_s}$ is the mean sample period of the randomly sampled signal. In our experiments, we set the decimation ratio $K = 10$. The GSM channels have a bandwidth equal to 200 kHz, so the bandwidth of the generated oversampled signal was equal to 2 MHz. We took into account the 10-th GSM band from 938.0 MHz to 940.0 MHz. We considered the busy band with central frequency equal to 939.0 MHz while left and right GSM channels have to be considered as interfering bands. To evaluate the performance of the proposed classification algorithms, we generated 1024 windows of signals whose length is equal to one half of the GSM timeslot. Operatively, we collected 547 samples per window from which we extracted randomly, in average, 55 samples in order to obtain the randomly sampled window and we extracted 1 sample every 10 in order to obtain the uniformly sampled signal. Each sequence of windows was generated in four different conditions: (1) no transmitted signal except noise in all the observed band; (2) a random generated information signal in the observed sub-band and noise in the remaining sub-bands; (3) a random generated information signal in the left sub-band adjacent to the observed one and noise in the observed band and in the remaining sub-bands; (4) a random generated information signal in the observed sub-band and in the left adjacent one and noise in all the remaining sub-bands. All the windows were generated in four different SNR conditions in each sub-band; specifically, we imposed an average SNR equal to 20 dB, 15 dB, 10 dB and 5 dB respectively. Globally, we generated and analyzed 16384 windows of signals.

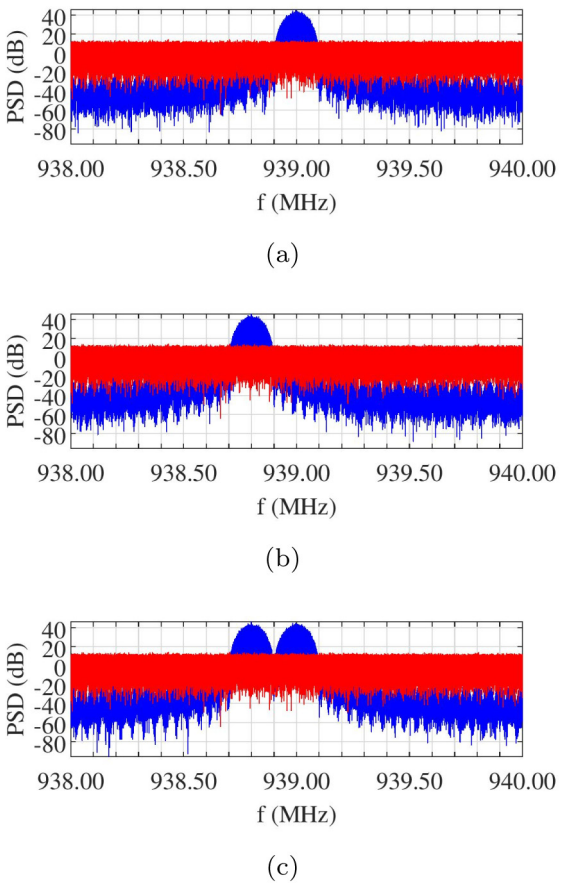

Fig. 5. PSD of oversampled signals (a) in-band, (b) out-band, (c) in-band/out-band (SNR=20 dB)

Fig. 5 shows the Power Spectral Density (PSD) of the white gaussian noise (red line) together with the PSD of the oversampled signals (the blue line) when it is an in-band signal only (Fig. 5(a)), an out-band signal only (Fig. 5(b)), and both an in-band and an out-band signal (Fig. 5(c)). Indeed, if downsampling is performed without filtering the desired sub-band, aliasing will affect the signal. In such a case, the Fourier transform of the downsampled signal Y will be related to original signal X according to the

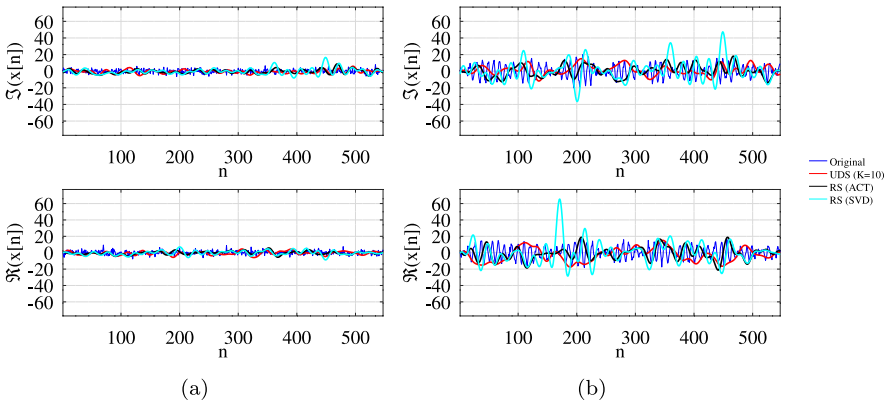

Fig. 6. Signal Rebuilding in presence of noise (a) and transmission on the left adjacent sub-band (b) at an SNR of 20 dB.

following relationship

$$Y(F) = \frac{1}{K}\sum_{k=0}^{K-1} X\left(\frac{F}{K} - \frac{k}{K}\right).$$

As already stated at the end of Section 3, in this work, we used JRS mode to emulate random sampling. Specifically, we added a discrete and uniformly distributed random variable $\tau \in \{0, \frac{1}{K}\cdot T_s, \ldots, \frac{K-1}{K}\cdot T_s\}$ to the original uniformly distributed sample instants. Therefore, we rebuilt the original signal using both SVD and ACT reconstruction approaches.

Fig. 6 shows a portion of the rebuilt signal using both uniform and random sampling when the signal is not present inside the observed sub-band. Specifically, Fig. 6(a) shows both real and imaginary components when in all the observed band only white gaussian noise is present, while Fig. 6(b) shows both real and imaginary rebuilt components when the sub-band adjacent to the left of the observed one is busy.

Fig. 7 shows a portion of the rebuilt signal using both uniform and random sampling when the signal is present inside the observed sub-band. Specifically, Fig. 7(a) shows both real and imaginary components when only the observed sub-band is busy, while Fig. 7(b) shows both real and imaginary rebuilt components when both the observed sub-band and the sub-band adjacent to the left of the observed one are busy.

Both Figs. 6 and 7 show the rebuilt signals when a white gaussian noise was added to the original one in such a way the average SNR level was 20 dB inside each active sub-band. Analysis of Fig. 7(a) shows that all the rebuilding approach works fine at this SNR level. Instead, as expected, all the rebuilding approaches fail when only noise is present (Fig. 6(a)) or the left channel is busy (Figs. 6(b) and 7(b)) due to the aliasing effect. Anyway, our goal is not the fidelity of the rebuilt signal to the original one but the ability to identify if the observed sub-band is busy or not. To this aim, we analyzed the time averaged PSD of the rebuilt signals using the three different approaches.

Fig. 8 shows the averaged PSDs when only noise is present in all the observed band 8(a), only the channel on the left of the observed one is busy 8(b), only the observed sub-band is busy 8(c) and, finally, when the observed channel and the left one are both busy 8(d). Comparing Fig. 8(b) with Fig. 8(c), it appears evident that the uniform downsampled (UDS) averaged PSD of the in-band signal is not distinguishable from the averaged PSD of the out-band signal, in fact the red graphs have a very similar shape; this is due to the aliasing effect. At the opposite, the use of random sampling rebuilding algorithms, in both SVD and ACT cases, produces reconstructed signals with some relevant differences, as the black and cyan lines in the two graphs put in evidence. Specifically, using SVD rebuilding, the curve trend inside the observed sub-band is quite flat when the in-band signal is not present, while it shows upwards concavity using the ACT rebuilding. Analyzing Fig. 8(d), it can be inferred that the averaged PSD evaluated by the UDS approach appears only slightly higher than the other cases, while the averaged PSD get with both the random sampling approaches continue to maintain relevant trend differences, meaning that UDS approach is less prone to be used for classification purposes.

In order to be able to classify the presence of the signal in the observed sub-band, we tried to capture these trend behavior in the one-shot PSD (using the FFT evaluated on only one window of the rebuilt signal). Specifically, we analyzed two different parameters: the average power in all the observed sub-band, and the ratio between the average power in the middle portion of the observed sub-band and the average power in the remaining portion of the observed sub-band; let us denote them P_a and ρ_p respectively. Fig. 9 shows the spreading of the two proposed parameters in the four different conditions where our analysis has been conducted: only noise (blue dot signs), out-band signal (red circle signs), in-band signal (yellow plus signs), and both out-band and in-band signals (purple times signs). Specifically, Fig. 9(a), Fig. 9(b) and Fig. 9(c) depict the behavior of the two parameters when the UDS, RS together with SVD, and RS together with ACT rebuilding algorithms were respectively used. The graphs point out that using the UDS approach the location of the points are particularly overlapped when the UDS approach is used and it is hard to distinguish the red circle signs by the yellow plus signs. Anyway the blue dot signs and purple time signs remain almost separated. At the opposite, using both RS approaches the sets of couple of parameters identifying the four working conditions remain separated. These results encouraged us in exploiting a machine learning approach for identifying free GSM slots.

5. Experimental classification results

Despite several classification approaches can be used (Linear Classifiers, Logistic Regression, Naive Bayes Classifier, Support Vector Machines, Decision Trees, Boosted Trees, Random Forest, Neural Networks, Nearest Neighbor), we decided to train and test a neural network to verify the possibility of discriminating the presence of the signal in the observed sub-band. Neural networks are a set of algorithms, considerably grown especially since the development of the first learning algorithm in 1985 [34]. They are now a classic tool for artificial intelligence (AI), and are widely used in classification tasks, evaluation of functions and optimization. They have the advantage of learning ability that makes them useful in problems for which there is no acceptable algorithmic solution. Moreover, their intrinsic parallelism gives

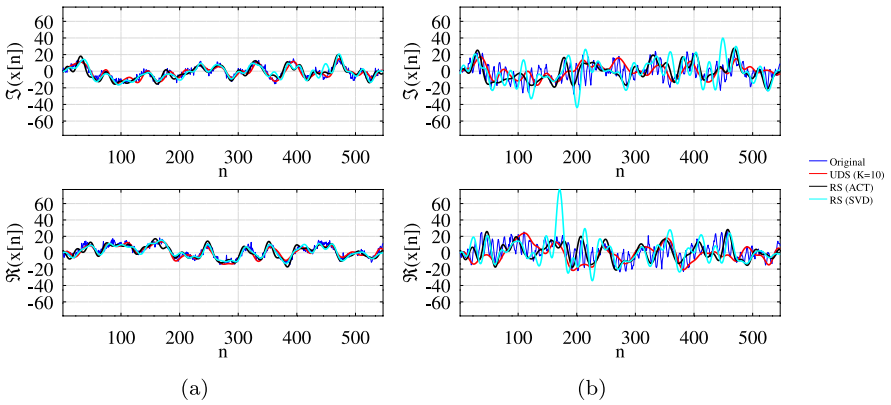

Fig. 7. Signal Rebuilding in presence of transmission in-band (a) and transmission both in-band and on the left adjacent sub-band (b) at an SNR of 20 dB.

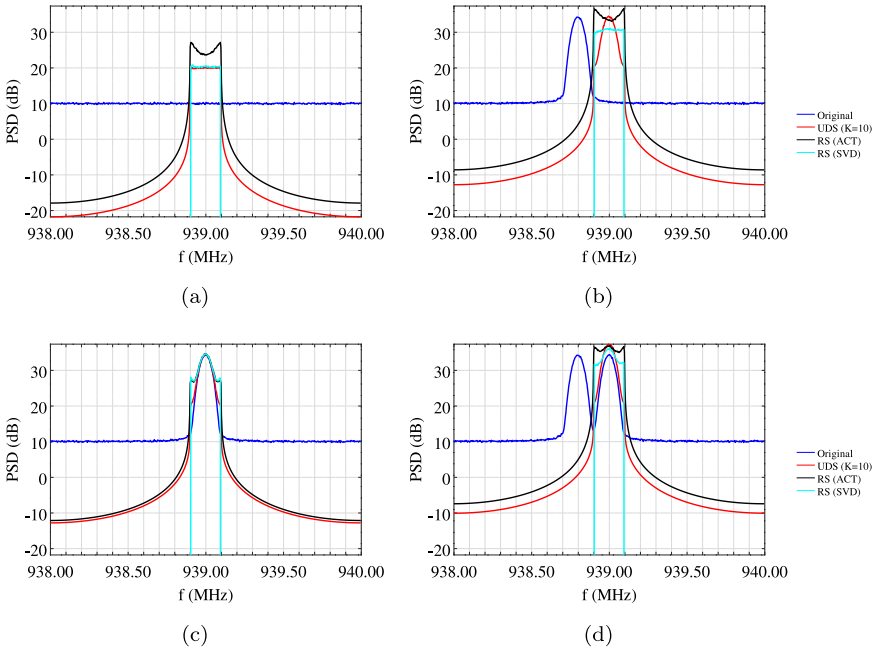

Fig. 8. PSD of the rebuilt signal in presence of only noise (a), transmission on the left adjacent sub-band (b), transmission only in-band (c) and transmission both in-band and on the left adjacent sub-band (d) at an SNR of 20 dB.

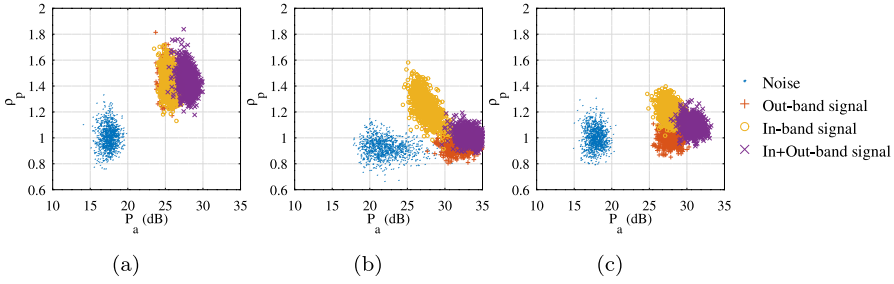

Fig. 9. Spreading of the proposed parameters using the considered rebuilding approaches with an SNR=20 dB (a) UDS, (b) SVD, (c) ACT.

them a great decision speed. They are widely used in areas such as recognition and prediction.

Several algorithms of artificial neural networks are proposed in the literature. Each model is characterized by its own architecture, treatment and rule of learning [35]. In our contribution, we were interested in multilayer perceptron (MLP). It has been used in system identification, time series prediction [36,37] and recently to perform multi-channel low-cost light spectrum measurement [38].

The MLP network is a multilayered structure consisting of an input layer, an output layer, and a few hidden layers. Excluding the input layer, every layer contains a certain number of computing units (referred to as neurons) which evaluate a weighted sum of input values and perform a nonlinear transform on the obtained sum. Neurons belonging to different layers are connected through adaptive weights.

Anyway the target of our work is to verify the capability of classifying the presence of the signal using random sampling

without focusing on the specific classification method to use for PUs detection. Instead, we want to show that a downsampling based technique together with the features introduced in Section 4 is effective. In fact, our purpose is to be able to evaluate the PUs detection in the context of slotted networks; thus, first of all, we need a sampling method fast enough for giving an accurate result within half timeslot. These required features introduce strict constraints in terms of sampling frequency and number of sampled data. That is why our choice fell to the random sampling technique that is the real subject of our research in this work, and we do not care about the efficiency of the classification method that is used only for testing the goodness of our choice. More formally, we want to discriminate between two hypotheses as defined in the following Eq. (13):

$$\begin{cases} \mathscr{H}_0 : y[n] = w[n] \\ \mathscr{H}_1 : y[n] = x_{PU}[n] + w[n] \end{cases} \tag{13}$$

Using the Octave [33] software package `nnets`, we trained an MLP for each SNR condition with 2 nodes in the input layer, 8 nodes in one hidden layer and 1 node in the output layer. The two input nodes will be filled up respectively with P_a and ρ_p parameters obtained as explained in Section 4. We used in all the nodes the `tansig` activation function and we trained the networks with half of the total set of data. As stated in Section 4, we generated 4096 signal windows, thus the total set of data consists of 4096 pairs of parameters (P_a, ρ_p) for each specific SNR condition.

Each MLP was trained in such a way its output value was equal to 1 when the input parameters (P_a, ρ_p) were extracted from a signal containing activity in the observed sub-band, meaning that it was busy; these working conditions arise in both "In-band" and "In-band/Out-band" signal conditions, as described in Section 4. On the other hand, the MLPs were trained setting the output value to -1 each time input values characterized a signal containing only noise in the sub-band, meaning that it is vacant; this latter case includes both "Noise" and "Out-band" signal conditions, as described in Section 4. We trained the MLPs using the backpropagation algorithm, specifically we used the Levenberg–Marquardt algorithm [39].

The number of examples used to train a MLP should be selected in order to obtain a good generalization of the problem. Training dataset size and dataset property itself plays an important role for the performance of the trained knowledge model. Anyway, as showed in [40], in many cases an increment in training dataset size does not produce a perceptible increment in accuracy as well; in fact, it is not ever used a training dataset size greater than one half of the original dataset size in [40]. The original dataset size contains 4096 examples for each specific couple of SNR and rebuilding algorithm in our experimentation. We split this set into three different disjoint subsets using the `subset` function of the `nnets` Octave package. This function randomly splits the rows of input data to train, test and validate the MLP. We used the default parameters of `subset` function, thus the training subset contained 50% of input data, whereas $^2/_3$ of the remaining data were used to build the testing subset and $^1/_3$ of them were available for the validation subset. Accordingly, we used 2048 randomly selected examples to build the training subset and 1365 randomly selected examples to build the testing subset for each specific working condition.

Before to start the training, we normalized the set of training data in order to obtain a set of input data with mean value equal to 0 and standard deviation equal to 1. Such a normalization was based, as usual, on the mean value and standard deviation of the set of training data. Since one input data was a couple (P_a, ρ_p), we derived the average values $\bar{P}_a$ and $\bar{\rho}_p$, and the standard deviations σ_{P_a} and σ_{ρ_p} of the set of training data; given a measured input data ($P_a^{(i)}$, $\rho_p^{(i)}$), the normalized value was been computed as

$$\left(\frac{P_a^{(i)} - \bar{P}_a}{\sigma_{P_a}}, \frac{\rho_p^{(i)} - \bar{\rho}_p}{\sigma_{\rho_p}} \right), \ i = 0, \ldots, 2047. \tag{14}$$

For consistency purposes, we used Eq. (14) to normalize also the input data during the testing phase. The mean square error (MSE) between the actual and the desired output was used as "performance function", with the goal of minimizing it. Each training phase of the MLP stopped either when the number of iterations exceeded 1000 epochs or the magnitude of the MSE gradient became less than 10^{-20}. The training time in our experimentation was set no longer than 1 hour. As shown in Fig. 10, all the MLPs converge after no more than 10 epochs due to the large number of examples used. However, using UDS approach, the MSE never drops below 0.5 (Figs. 10(a)–10(d)), while using both SVD and ACT approaches, it does not drop below 0.5 only for SNRs lower than 15 dB (Figs. 10(e)–10(h) and Figs. 10(i)–10(l)). These results are in accordance with those shown in Fig. 8 which show it is not possible to distinguish between PSDs obtained during transmissions in-band and PSDs obtained during transmissions on the left adjacent sub-band when UDS is used. This result is also in accordance with the graphs shown in Fig. 9 where the scatter diagrams of the two parameters (P_a, ρ_p) used for classification are depicted; it is easy to see that the areas identifying different band occupancy states are almost completely superposed when UDS is used, while they are partially separated in case of RS together with both SVD and ACT as a rebuilding algorithm. Each graph shows the trend of MSE for both training examples and validation examples during the first 50 epochs. All the MLP trainings finished because the MSE gradient fell below 10^{-20} during the performed experimentation.

Figs. 11(a)–11(d) show the results of MLP classification test in terms of distribution of the output values using uniform downsampling and considering the four different SNRs conditions. As we expected, the MLPs were not able to obtain the right classification even at the highest SNR. Figs. 11(e)–11(h) show the results of MLP classification test using SVD rebuild. The graphs put in evidence a good separation of the two classes both at 20 dB and 15 dB of SNRs, instead they appear almost overlapped for lower SNR values. Using the ACT rebuilding approach (Figs. 11(i)–11(l)), the test behaves better, in fact a good separation of the two classes is obtained for all the SNR levels except at 5 dB when they become almost overlapped.

In order to perform the classification into a production environment, we need a threshold *Th* for comparing with the output of the MLP (MLP_O) and making a decision about which of the two hypotheses holds. Based on how we trained the MLP, we looked for a threshold such that if $MLP_O \geq Th$ the sub-band is considered busy, otherwise it is assumed into a vacant condition. The threshold value can be set accordingly to desired specifications in term of *right detection* or *false-alarm* probability of the busy condition in the observed sub-band.

To better highlight the improvement using the random sampling approaches, we evaluated and plotted the Receiver Operating Characteristic (ROC) curves at the different SNRs (Fig. 12), where false alarm probability P_{FA} and correct detection probability P_D are depicted changing the threshold value. Figs. 12(a) and 12(b) show it is possible to considerably increase the performances of classification using both the random sampling approaches. Specifically, ACT outperforms SVD and it is possible to obtain a false alarm probability lower than 20% maintaining the detection probability close to 100%. Performances degrade at 10 dB SNR although both ACT and SVD outperform UDS. When the SNR level is equal to 5 dB (Fig. 12(d)), the use of random sampling

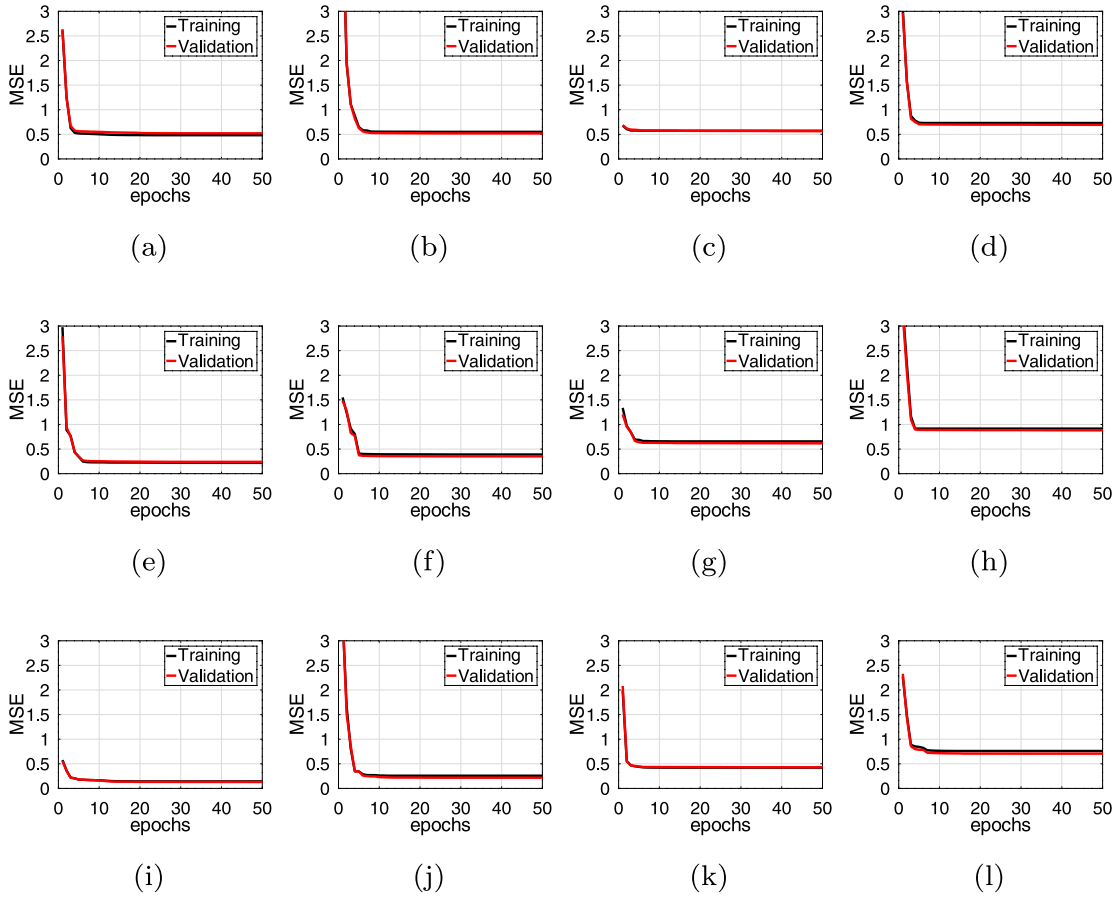

Fig. 10. MLPs performance in terms of MSE versus training epochs using UDS rebuilding [(a) 20 dB, (b) 15 dB, (c) 10 dB, (d) 5 dB], RS and SVD rebuilding [(e) 20 dB, (f) 15 dB, (g) 10 dB, (h) 5 dB], RS and ACT rebuilding [(i) 20 dB, (j) 15 dB, (k) 10 dB, (l) 5 dB].

appears useless, specifically ACT obtains the same performances of UDS while SVD behaves worse than the previous ones.

When the right detection of "busy condition" is the main application requirement (like in our cognitive radio application), we want a threshold such that the probability of right detection is equal to 1.0 keeping at the same time the false alarm probability as low as possible; this implies that the SUs never interfere with PUs. Using the RS (ACT) approach, it is possible to find a threshold such that $P_D = 1.0$ and $P_{FA} = 0.2$ when SNR level is 20 dB, and $P_D = 1.0$ and $P_{FA} = 0.3$ when SNR level is 15 dB. In these SNRs conditions, the performances of the RS system would be double in terms of throughput because the minimum false alarm probability value to obtain $P_D = 1.0$ is $P_{FA} = 0.5$ using the UDS approach. It is noteworthy we perform the classification of the spectrum status taking into account only a single observation of the signals and a window size equal to half a single GSM timeslot. This is the main difference of the method here discussed with respect the other works that have better performance at lower SNRs. In fact, in order to obtain good performance at lower SNRs, it is necessary to increase the number of observations, i.e. the number of signal windows observed to perform the classification [41]. Specifically, the authors of [41] use a Cyclostationary Approach to perform signal Classification. For example they show that in order to obtain a detection probability greater than 90% with 10% as false alarm rate at -3 dB more than 50 observations are necessary. Specifically each observation consists of $N = 100$ samples, thus at least 5000 samples have to be used. Also using the Multi-Coset approach like in [19], the authors use a number of samples much greater than those we use for our approach to obtain good performance at low SNR: specifically they used 163840 samples (this number was obtained as $p \cdot M \cdot K$, with $p = 10$, $M = 512$ and $K = 32$ parameters in eq. (10) of [19]). In our approach, we use only 55 samples randomly extracted in a period equal to the half time of one GSM timeslot when we perform the classification. It is important to remind at this point that the goal of our work is the classification of the busy/free state of the spectrum within a time equal to at most half of a single GSM timeslot. In fact the SU accesses the channel only when it does not reveal the presence of PU transmission. In this condition, to preserve the destruction of PU information, it is mandatory to obtain a high probability of detection. Moreover, a high false alarm probability value means the SU will not access the channel with the specified probability also when the PU is not transmitting. In this latter condition the SU observes a degradation of the maximum available rate. As Fig. 13 shows, the proposed RS approaches permit to obtain an increment of detection probability compared with results obtained with UDS. Specifically, if a false alarm probability equal to 10% (Fig. 13(a)) is required by the application, the RS-ACT approach permits to obtain a probability of detection higher than 80% starting from a SNR equal to 10 dB. In particular, as shown in Fig. 13(b), if a false alarm probability equal to 40% is satisfactory, the RS-ACT approach allows to obtain a detection probability near to 100% starting from an SNR equal to 10 dB. This means that in these conditions the SU could access the channel without ever interfering with the PU and with a transmission rate equal to 60% of the maximum available.

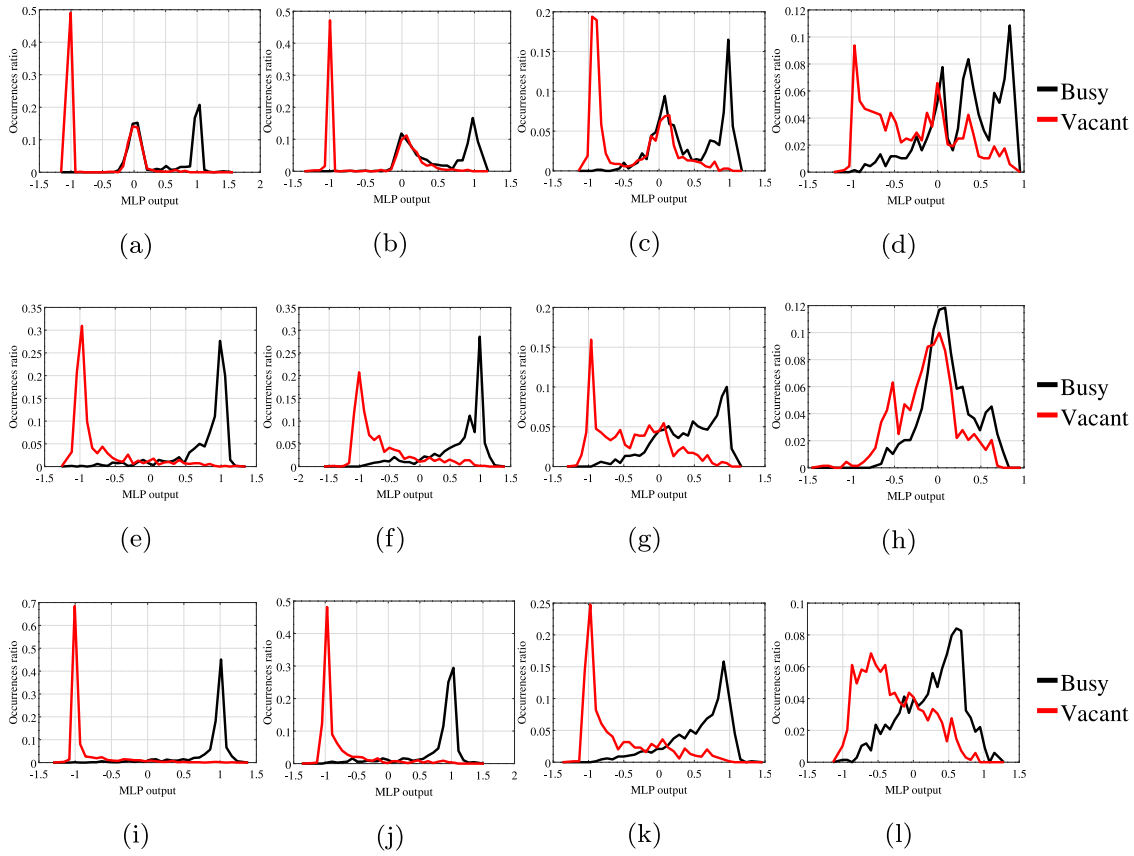

Fig. 11. MLP output distribution using UDS rebuilding [(a) 20 dB, (b) 15 dB, (c) 10 dB, (d) 5 dB], RS and SVD rebuilding [(e) 20 dB, (f) 15 dB, (g) 10 dB, (h) 5 dB], RS and ACT rebuilding [(i) 20 dB, (j) 15 dB, (k) 10 dB, (l) 5 dB].

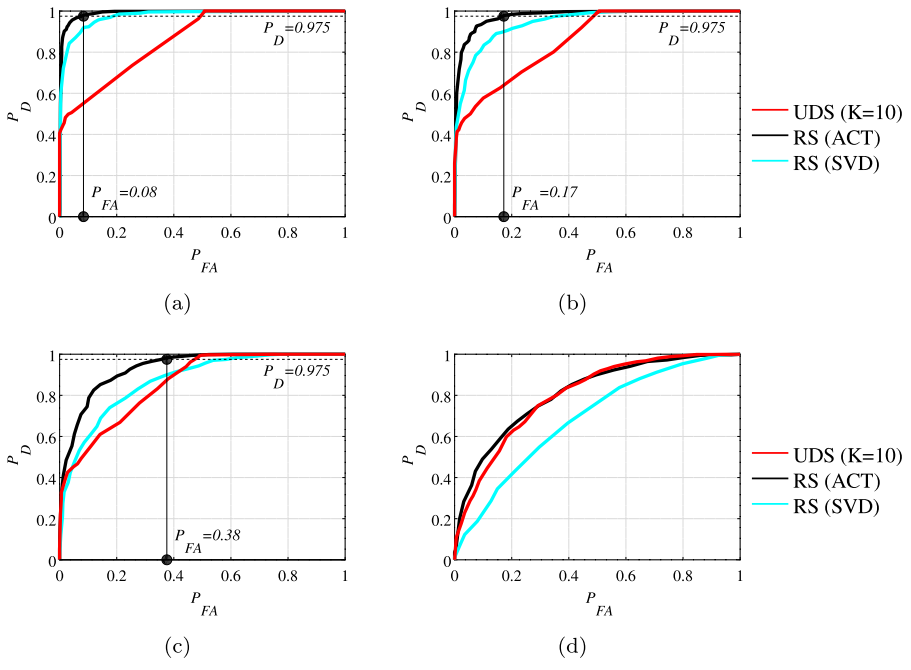

Fig. 12. ROC curves [(a) 20 dB, (b) 15 dB, (c) 10 dB, (d) 5 dB].

6. Conclusions

Actually, the cognitive radio is considered as an exceptional innovation being used in modern wireless communications. In this work, our interest was the spectrum sensing which represents the main function in a CR system. Thus, we introduced the implementation of the SS function based on GSM Signal using random sampling technique. The proposed application is evaluated in terms of the detection of the presence or absence of the

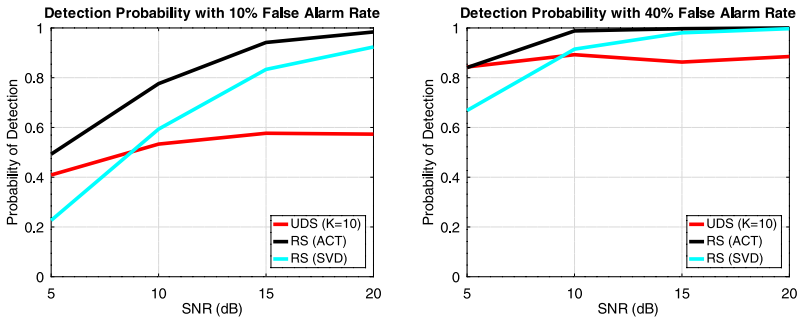

Fig. 13. Detection Probability of (a) 10% False Alarm and (b) 40% False Alarm.

activity in the GSM channel using synthetically generated signals at different SNRs. A set of two parameters obtained from the PSD of the rebuilt signal was introduced to perform this detection. A machine learning approach based on neural networks was used to perform decisions on spectrum occupancy. The obtained experimental results show that random sampling associated with machine learning approach represents an interesting solution in cognitive radio systems comparing to the uniform sampling case. Specifically, the proposed approach permits to perform spectrum sensing also in an environment characterized by fast variations of the channel occupancy state.

CRediT authorship contribution statement

Salvatore Serrano: Conceptualization, Methodology, Software, Investigation, Formal analysis, Writing – original draft, Writing – review & editing. **Marco Scarpa:** Conceptualization, Methodology, Software, Investigation, Writing – original draft, Writing – review & editing. **Asmaa Maali:** Conceptualization, Methodology, Writing – original draft. **Abdallah Soulmani:** Conceptualization, Writing – original draft. **Najib Boumaaz:** Conceptualization, Writing – original draft.

Declaration of competing interest

The authors declare that they have no known competing financial interests or personal relationships that could have appeared to influence the work reported in this paper.

Acknowledgments

This work was done as part of a research internship funded by the European Union under the Erasmus+ Program. Authors would like to thank this organization for their support.

References

[1] G. Kakkavas, K. Tsitseklis, V. Karyotis, S. Papavassiliou, A software defined radio cross-layer resource allocation approach for cognitive radio networks: From theory to practice, IEEE Trans. Cogn. Commun. Netw. 6 (2) (2020) 740–755.
[2] A. Maali, H. Semlali, N. Boumaaz, A. Soulmani, Energy detection versus maximum eigenvalue based detection: A comparative study, in: 2017 14th International Multi-Conference on Systems, Signals & Devices, SSD, IEEE, 2017, pp. 1–4.
[3] H. Semlali, N. Boumaaz, A. Soulmani, A. Ghammaz, J.-F. Diouris, Energy detection approach for spectrum sensing in cognitive radio systems with the use of random sampling, Wirel. Pers. Commun. 79 (2) (2014) 1053–1061.
[4] H. Semlali, A. Maali, N. Boumaaz, A. Soulmani, A. Ghammaz, J.-F. Diouris, Spectrum sensing operation based on a real signal of FM radio: Feasibility study using a random sampling mode, in: 2016 International Conference on Information Technology for Organizations Development, IT4OD, IEEE, 2016, pp. 1–4.
[5] Cognitive radio for public safety, 2018, URL https://www.fcc.gov/general/cognitive-radio-public-safety.
[6] A. Ali, W. Hamouda, Advances on spectrum sensing for cognitive radio networks: Theory and applications, IEEE Commun. Surv. Tutor. 19 (2) (2017) 1277–1304, http://dx.doi.org/10.1109/COMST.2016.2631080.
[7] S. Kusaladharma, C. Tellambura, An overview of cognitive radio networks, Wiley Encyclopedia Electr. Electron. Eng. (1999) 1–17.
[8] M. Scarpa, S. Serrano, A full secondary user model for cognitive radio in a GSM-900 scenario, in: 2019 International Conference on Computing, Networking and Communications, ICNC, 2019, pp. 344–349.
[9] A. Maali, S. Laafar, H. Semlali, N. Boumaaz, A. Soulmani, Maximum eigenvalue based detection using jittered random sampling, in: International Conference on Wireless Intelligent and Distributed Environment for Communication, Springer, 2018, pp. 183–191.
[10] V.K. Tumuluru, P. Wang, D. Niyato, A neural network based spectrum prediction scheme for cognitive radio, in: 2010 IEEE International Conference on Communications, IEEE, 2010, pp. 1–5.
[11] L. Yin, S. Yin, W. Hong, S. Li, Spectrum Behavior Learning in Cognitive Radio Based on Artificial Neural Network, Military Communication Conference, Track 1, Waveforms and Signal Processing, IEEE, 2011.
[12] A. Agarwal, S. Dubey, M. Khan, R. Gangopadhyay, S. Debnath, Learning based primary user activity prediction in cognitive radio networks for efficient dynamic spectrum access, in: 2016 International Conference on Signal Processing and Communications, SPCOM, 2016, pp. 1–5, http://dx.doi.org/10.1109/SPCOM.2016.7746632.
[13] J.J. Wojtiuk, R.J. Martin, Random sampling enables flexible design for multiband carrier signals, IEEE Trans. Signal Process. 49 (10) (2001) 2438–2440.
[14] A. Sahai, Spectrum sensing: fundamental limits and practical challenges, in: Tutorial Document on DySPAN 2005, Nov., 2005.
[15] T. Sun, J. Li, P. Blondel, Direct under-sampling compressive sensing method for underwater echo signals and physical implementation, Appl. Sci. 9 (21) (2019) 4596.
[16] R. Venkataramani, Y. Bresler, Optimal sub-nyquist nonuniform sampling and reconstruction for multiband signals, IEEE Trans. Signal Process. 49 (10) (2001) 2301–2313, http://dx.doi.org/10.1109/78.950786.
[17] M. Mishali, Y. Eldar, From theory to practice: Sub-nyquist sampling of sparse wideband analog signals, IEEE J. Sel. Top. Sign. Proces. 4 (2) (2010) 375–391, http://dx.doi.org/10.1109/JSTSP.2010.2042414.
[18] D. Arianandа, G. Leus, Z. Tian, Multi-coset sampling for power spectrum blind sensing, in: 2011 17th International Conference on Digital Signal Processing, DSP, 2011, pp. 1–8, http://dx.doi.org/10.1109/ICDSP.2011.6005003.
[19] S. Traoré, B. Aziz, D. Le Guennec, Y. Louet, Adaptive non-uniform sampling of sparse signals for green cognitive radio, Comput. Electr. Eng. 52 (2016) 253–265.
[20] F. Salahdine, N. Kaabouch, H. El Ghazi, A survey on compressive sensing techniques for cognitive radio networks, Phys. Commun. 20 (2016) 61–73.
[21] G. Aswathy, K. Gopakumar, Sub-nyquist wideband spectrum sensing techniques for cognitive radio: A review and proposed techniques, AEU-Int. J. Electron. Commun. 104 (2019) 44–57.
[22] A. Deutsche Telecom, Narrowband IoT groundbreaking in the internet of things, 2017, https://www.b2b-europe.telekom.com/downloads/Telekom-B2B-NBIOT_whitepaper.pdf?20180723125459.
[23] K.P. Patil, S. Barge, K.E. Skouby, R. Prasad, Spectrum occupancy information in support of adaptive spectrum sensing for cognitive radio, Netw. Protocols Algorithms 6 (1) (2014) 76–86.
[24] S. El Barrak, A. El Gonnouni, S. Serrano, A. Puliafito, A. Lyhyaoui, GSM-RF Channel characterization using a wideband subspace sensing mechanism for cognitive radio networks, Wirel. Commun. Mobile Comput. 2018 (2018).

[25] H. Technologies, Narrowband IoT: Wide range of opportunities, in: Mobile World Congress 2016, 2016, http://www-file.huawei.com/-/media/CORPORATE/minisite/mwc2016/pdf/NarrowBand-IoT-Wide-Range-of-Opportunities-en.pdf?la=en.
[26] Beutler, Error free recovery of signals from irregularly spaceed samples, SIAM REV. (1966).
[27] Wojtiuk, Randomized Sampling for Radio Design (Ph.d. thesis, Ph.D.), University of South Australia, 2001.
[28] F. Marvasti, Nonuniform Sampling: Theory and Practice, Springer Science & Business Media, 2012.
[29] H.S. Shapiro, R.A. Silverman, Alias-free sampling of random noise, J. Soc. Ind. Appl. Math. 8 (2) (1960) 225–248.
[30] H. Semlali, Développement de nouvelles structures et d'algorithmes appliquant l'échantillonnage aléatoire pour des systèmes de types radio logicielle et radio cognitive (Ph.D. thesis), UNIVERSITE DE NANTES, 2015.
[31] T. Strohmer, E Cient Methods for Digital Signal and Image Reconstruction from Nonuniform Samples (Ph.D. thesis), Ph.D. thesis, Institut f ur Mathematik der Universit at Wien, 1993.
[32] H.G. Feichtinger, K. Gr, T. Strohmer, et al., Efficient numerical methods in non-uniform sampling theory, Numer. Math. 69 (4) (1995) 423–440.
[33] J.W. Eaton, D. Bateman, S. ren Hauberg, R. Wehbring, GNU Octave version 5.2.0 manual: a high-level interactive language for numerical computations, 2020, URL https://www.gnu.org/software/octave/doc/v5.2.0/.
[34] G. Rubino, P. Tirilly, M. Varela, Evaluating users' satisfaction in packet networks using random neural networks, in: International Conference on Artificial Neural Networks, Springer, 2006, pp. 303–312.
[35] M. Abadi, Réalisation d'un réseau de neurones" SOM" sur une architecture matérielle adaptable et extensible à base de réseaux sur puce" NoC" (Ph.D. thesis), Université de Lorraine; Université du Centre (Sousse, Tunisie), 2018.
[36] K. Narendra, K. Parthasarathy, Identification and control of dynamical systems using neural networks, IEEE Trans. Neural Netw. 1 (1) (1990) 4–27, http://dx.doi.org/10.1109/72.80202.
[37] P. Werbos, Backpropagation through time: what it does and how to do it, Proc. IEEE 78 (10) (1990) 1550–1560, http://dx.doi.org/10.1109/5.58337.
[38] J.-S. Botero-Valencia, J. Valencia-Aguirre, D. Durmus, W. Davis, Multi-channel low-cost light spectrum measurement using a multilayer perceptron, Energy Build. 199 (2019) 579–587, http://dx.doi.org/10.1016/j.enbuild.2019.07.026, URL http://www.sciencedirect.com/science/article/pii/S0378778819309788.
[39] J.J. Moré, The levenberg-marquardt algorithm: Implementation and theory, in: G.A. Watson (Ed.), Numerical Analysis, Springer Berlin Heidelberg, Berlin, Heidelberg, 1978, pp. 105–116.
[40] H. Sug, The effect of training set size for the performance of neural networks of classification, WSEAS Trans. Comput. 9 (9) (2010) 1297–1306.
[41] K. Kim, I.A. Akbar, K.K. Bae, J.-S. Um, C.M. Spooner, J.H. Reed, Cyclostationary approaches to signal detection and classification in cognitive radio, in: 2007 2nd IEEE International Symposium on New Frontiers in Dynamic Spectrum Access Networks, IEEE, 2007, pp. 212–215.

Salvatore Serrano received the degree in computers engineering and Ph.D. degree in computers and telecommunications engineering from the University of Catania, Italy, in 1999 and 2003, respectively. Currently he is with the Department of Engineering at the University of Messina, as researcher and Assistant Professor. His research interests are in the fields of digital signal processing, speech and audio signal processing and coding, speech and speaker recognition, biomedical signal processing, data mining, voice over IP, and wired and wireless communications systems.

Marco Scarpa received the degree in Computer Engineering in 1994 and Ph.D. on Computer Science from University of Turin in February 2000. He is currently Associate Professor of Computer Engineering at University of Messina. He is stable referee of several international conferences and computer science journals such as: "IEEE Transactions on Dependable and Secure Computing", "IEEE Transactions on Parallel and Distributed Systems", "International Journal of System and Sciences", "Performance Evaluation", "Journal of Computational Science", and many others. He served as guest editor of a special issue of Performance Evaluation (Elsevier); he is currently editorial board member of the Journal of Distributed Sensor Network" and Area Editor of EAI Transactions on Cloud Systems. He has been involved in many Technical Program Committees of international conference. His research activity includes reliability and availability analysis of distributed systems, wireless sensor networks, algorithms for management of opportunistic access in cognitive radio systems, algorithms for solution of non Markovian stochastic Petri net, phase type distributions, and software performance evaluation techniques especially applied to distributed systems. Recently, he started a collaboration with industries in efficient music recognition algorithms field. He has been actively involved in several research projects. He coordinates the developments of WebSPN, a software tool able to manage stochastic Petri nets with generally distributed firing times for the study of system performances and reliability, and MAGNET, a C/C++ software library providing easy management and implementation of complex Markovian Agent based models.

Asmaa Maali received the Bachelor degree in Network and Telecommunications from Hassan II University, Casablanca, Morocco, in 2011. In 2013, she received the Master degree in Network and Telecommunications from Chouaib doukkali University, Eljadida, Morocco. She is pursing the Ph.D. degree at the Department of Applied Physics as a candidate in Electrical Systems and Telecommunications Laboratory of Faculty of Sciences and Technologies of Cadi Ayyad University, Marrakech, Morocco. His current research interests includes Telecommunications, signal processing, signal sampling and Cognitive Radio. (Email: maali.asmaa@gmail.com).

Abdallah Soulmani is born in 1970. He received his Engineer Diploma in Electronics from the Polytechnic School of the University of Nantes in 1994. He joined the High School of Technology of Safi (EST Safi) as a Professor. In 2003, he received his Ph.D. in Electronics and Telecommunications from the University of Nantes, France. His research interests cover software radio architectures and random sampling. (Email: a.soulmani@uca.ma).

Najib Boumaaz received the B.Tech. degree in electronics from Normal High School for Professor of Technology of Mohammedia (ENSET), Morocco and the M.S from University Cadi Ayyad of Marrakech, Morocco. In 2008, he received his Ph.D. in electronic from the Polytechnic School of Nantes, France. He is currently an Assistant-Professor at the High School of Technology in Safi, Morocco. His research interests include electronics, telecommunications, statistical signal processing, signal sampling and interpolation. (Email: n.boumaaz@gmail.com).